Charge regulation triggers condensation of short oligopeptides to polyelectrolytes

Sebastian P. Pineda,[†] Roman Staňo,[‡,¶] Anastasiia Murmiliuk,[§] Pablo M. Blanco,[‖,†,⊥] Patricia Montes,[†] Zdeněk Tošner,[†] Ondřej Groborz,[#] Jiří Pánek,[#] Martin Hrubý,[#] Miroslav Štěpánek,[*,†] and Peter Košovan[*,†]

†*Department of Physical and Macromolecular Chemistry, Faculty of Science, Charles University, Hlavova 8, 128 40 Prague 2, Czech Republic*

‡*Faculty of Physics, University of Vienna, Boltzmanngasse 5, 1090 Vienna, Austria*

¶*Vienna Doctoral School in Physics, University of Vienna, Boltzmanngasse 5, 1090 Vienna, Austria*

§*Jülich Centre for Neutron Science JCNS at Heinz Maier-Leibnitz Zentrum (MLZ), Forschungszentrum Jülich GmbH, Lichtenbergstraße 1, 85748 Garching, Germany*

‖*Department of Material Science and Physical Chemistry, Research Institute of Theoretical and Computational Chemistry (IQTCUB), University of Barcelona, C/Martí i Franquès 1, 08028 Barcelona, Spain*

⊥*Department of Physics, NTNU - Norwegian University of Science and Technology, NO-7491 Trondheim, Norway*

#*Institute of Macromolecular Chemistry AS CR, Heyrovský square 2, 162 06 Prague 6, Czech Republic*

E-mail: miroslav.stepanek@natur.cuni.cz; peter.kosovan@natur.cuni.cz

Abstract

Electrostatic interactions between charged macromolecules are ubiquitous in biological systems and they are important also in materials design. Attraction between oppositely charged molecules is often interpreted as if the molecules had a fixed charge, which is not affected by their interaction. Less commonly, charge regulation is invoked to interpret such interactions, *i.e.*, a change of the charge state in response to a change of the local environment. Although some theoretical and simulation studies suggest that charge regulation plays an important role in intermolecular interactions, experimental evidence supporting such view is very scarce. In the current study, we used a model system, composed of a long polyanion interacting with cationic oligolysines, containing up to 8 lysine residues. We showed using both simulations and experiments that while these lysines are only weakly charged in the absence of the polyanion, they charge up and condense on the polycations if the pH is close to the pKa of the lysine side chains. We show that the lysines coexist in two distinct populations within the same solution: 1. practically non-ionized and free in solution; 2. highly ionized and condensed on the polyanion. Using this model system, we demonstrate under what conditions charge regulation plays a significant role in the interactions of oppositely charged macromolecules and generalize our findings beyond the specific system used here.

Keywords: *charge regulation; counterion condensation; polyelectrolyte complexes; electrostatic association; constant pH Monte Carlo; potentiometric titration; pKa; NMR titration.*

Introduction

Charged moieties are omnipresent in aqueous environments in both natural and synthetic worlds. From small monoatomic ions up to complex molecules with multiple charges, such as proteins, the interactions between such ionic groups are governed mainly by a Coulomb potential, which is non-specific, non-covalent and long ranged. The above interactions are vital

for living matter; for instance, they provide the driving force for complexation of DNA with positively charged histones,[1,2] compaction of viral genome,[3] assembly of actin filaments into bundles by multivalent binders[4] or formation of complex coacervates[5,6] and membraneless organelles.[7] Ample biopolymers such as RNA, DNA, hyaluronic acid or many intrinsically disordered proteins bear charged groups,[8–10] which provide unique means of their regulation and organization through changes of pH, type of salt ions or their concentration. There have been attempts to utilize the above responsiveness in design of inverse patchy colloids,[11,12] in supramolecular engineering,[13–15] peptide nanotechnology[16–18] or gene delivery.[19,20] For example, adhesion of highly cationic lysozyme to the anionic bacterial cell wall is important for its bactericidal effect.[21] Another example is the penetration of SARS-CoV-2 into cells, which is crucially determined by the multivalent charge interaction[22] of the cationic domains of the spike protein with polyanions on the glycocalyx of the target cells. Accordingly, its entry into the cell can be inhibited by employing polyanions binding to the cationic part of the spike protein or by small oligocations that mask the negative charge of the glycocalyx.[23,24] Nevertheless, to harvest such applications, we first need better fundamental understanding of the electrostatic interaction and its mediation by charge regulation, *i.e.*, by a change in the charge state in response to changes in the pH or in other parameters of the local environment.

Although it is generally known that oppositely charged molecules attract each other, it is not easy to tell under what conditions their attraction is strong enough, so that they associate. The term counterion condensation has been coined to describe such interaction in polyelectrolyte solutions. According to the early theory of Manning, counterions should condense on an oppositely charged polyelectrolyte chain until they reduce its effective linear charge density to a threshold value.[25–28] Notably, in this context we use the term counterion not only for small monovalent ions but more generally for any oppositely charged ions or molecules present in the solution. The threshold charge density for monovalent counterions amounts to one elementary charge per Bjerrum length. At the threshold charge density, the loss in their translational entropy upon condensation is compensated by the enthaply gain

due to electrostatic interactions. The condensed counterions are confined to the vicinity of the polyelectrolyte which is manifested by a lower osmotic pressure of the solution.[29] The mobility of condensed counterions is significantly reduced because of the confinement, however, they remain sufficiently mobile to dynamically escape from the confinement at the chain. Sometimes, the term counterion condensation is used to describe simple accumulation of counterions near polyelectrolytes by other mechanisms than electrostatic interactions, *e.g.*, due to ion-specific effects, also in situations when the Manning conditions for counterion condensation are not met.[30,31] Although we acknowledge that these ion-specific effects may be important, in further discussion we will focus on electrostatic effects, which become dominant if multivalent or oligomeric ions are present in the system.

If multivalent counterions are present in a mixture with monovalent ions, then the multivalent ones condense first, while the monovalent ones remain free. This is because a multivalent counterion of valency z loses the same amount of translational entropy as a monovalent one, whereas it gains z-times more electrostatic energy upon condensation. Therefore, the condensation threshold for z-valent counterions can be estimated to be z-times lower than for the monovalent ones. Alternatively, one can argue that if a z-valent counterion condenses on a polyelectrolyte, it displaces z monovalent counterions which are released into the solution. The released counterions gain translational entropy $T\Delta S = (z-1)k_{\mathrm{B}}T$, which is the main driving force of the condensation. In contrast, the net change in electrostatic interaction energy is small, resulting in $\Delta H \approx 0$. Therefore, if multivalent counterions are present, then practically all of them condense, displacing the monovalent ones which remain mostly free. Thermodynamic analysis of experimental data,[32,33] supported by simulations,[34,35] shows that the entropy gain due to counterion release[32–34] and solvent reorganization[35,36] are the main driving forces of condensation of multivalent counterions, whereas the contribution due to polymer-ion electrostatic interactions seems to be less significant. The condensation of multivalent counterions is used, *e.g.*, for the compaction of DNA by cationic poly(ethyelene imine),[37,38] spermine or spermidine,[39] and the same physics can be used to describe the

binding of DNA to positively charged histones.[1,2] The formation of interpolyelectrolyte complexes upon mixing of two oppositely charged polyelectrolytes can be viewed as an extreme case of counterion condensation, also being driven by the release of monovalent ions.[40,41] For example, the interaction of long polyelectrolytes with short oligomeric counterions could be described as both, counterion condensation or polyelectrolyte complexation. However, one would probably describe it as counterion condensation only if the counterions are much smaller than the polymer and they are present in a much smaller amount. A higher amount of oligomeric counterions would likely result in precipitation and formation of clusters involving multiple polymer chains. In this case, it would be described as polyelectrolyte complexation. Nonetheless, if the association of two oppositely charged molecules is accompanied by significant conformational changes, such as the compaction of DNA or polyelectrolyte complexation, then not only electrostatics but also other specific interactions may contribute to the net effect.

If weakly acidic or basic groups are involved in the interaction between two oppositely charged molecules, they can undergo charge regulation, *i.e.*, a change in their ionization states as a response to a change in their local environment. The charge regulation in polyelectrolytes composed of identical monomers (polyacids or polybases) decreases their net charge in order to decrease the electrostatic repulsion among like-charged groups. Consequently, charge regulation shifts the effective $\mathrm{p}K_\mathrm{A}$ of polyacids to higher values and the effective $\mathrm{p}K_\mathrm{A}$ of polybases to lower values than those of the corresponding monomers.[42,43] Charge regulation in peptides, proteins or synthetic polyampholytes, which contain both acidic and basic groups, may shift the effective $\mathrm{p}K_\mathrm{A}$ of these groups in either direction, depending on what kind of charges prevail and how they are distributed in space.[44–51]

Within the mean-field picture, the degree of ionization, α, can be described by the Henderson-Hasselbalch equation, augmented by an additional electrostatic term[52–54]

$$\mathrm{pH} - \mathrm{p}K_\mathrm{A} = \log_{10} \frac{1-\alpha}{\alpha} + \frac{ze\psi}{k_\mathrm{B}T \ln 10} \tag{1}$$

where e is the elementary charge, $z = \pm 1$ is the valency of the ionized group and ψ is the local electrostatic potential. In the absence of interactions (ideal gas limit), $\psi = 0$, therefore, 50% of the groups in the molecules are ionized ($\alpha = 0.5$) at pH = pK_{A}. The shift of the effective pK_{A} then follows as $\mathrm{p}K_{\mathrm{A}}^{\mathrm{eff}} = \mathrm{p}K_{\mathrm{A}} + (ze\psi)/(k_{\mathrm{B}}T \ln 10)$.[52]

Several theoretical studies suggested that charge regulation may significantly contribute to interactions between two oppositely charged macromolecules. Simulations by Rathee *et al.*.[55] predicted by simulations that if a polyacid and polybase interact while the solution pH is close to the pK_{A} of one of them, then that molecule charges up to make the attraction more favourable. They termed this effect "strong associative charging", in contrast to "weak associative charging" which occurs if the pH is close to the pK_{A} of both these molecules, so that they both simultaneously charge up upon interaction. In accordance with that, Staňo *et al.*[56] predicted by simulations that charge regulation may enable the formation of electrostatically crosslinked gels at a pH value when one of the interacting macromolecules would be uncharged in the absence of its oppositely charged interaction partner. This theoretical prediction seems to explain why some experiments[57,58] observed complexation of charge-regulating polyelectrolytes at pH values when these polyelectrolytes should not yet be sufficiently charged. The same mechanism could explain the binding of short DNA to supramolecular polymers containing mobile cationic moieties.[59] Along these lines, simulations by Staňo suggested that short oligopeptides could increase their net charge when interacting with oppositely charged polyelectrolytes, such as DNA.[60] Subsequently, Lunkad *et al.*[61] have shown that if peptides interact with polyelectrolytes, then charge regulation may allow the peptides to switch the sign of their net charge, provided that pK_{A} values of acidic or basic groups on the peptide are close to the solution pH. The simulation study by Lunkad *et al.*[61] provided an alternative explanation of why proteins adsorb on polyelectrolytes on the "wrong" side of the isoelectric point, *i.e.*at pH values when the net charge of the protein has the same sign as the polyelectrolyte. Previously, this phenomenon has been explained by the release of counterions, enabled by patchy charge distribution on the

protein.[62] Interestingly, the effect of charge regulation could be interpreted so that it facilitates the formation of oppositely charged patches, thus enabling attraction of the protein to the oppositely charged macromolecule, accompanied by the release of monovalent counterions. Therefore, although most experiments can be quantitatively described by counterion release, it does not exclude the possibility that charge regulation plays an important role. Interestingly, the important role of charge regulation has been demonstrated in the studies of phase-separating systems forming interpolyelectrolyte complexes or polyelectrolyte multilayers. In these systems, highly ionized and weakly ionized forms of the same molecule have been found to coexist at equilibrium in two different phases, which provide different microenvironments for the charge-regulating species.[63–68] More specifically, these studies have shown that the ionization is enhanced in the polyelectrolyte phase. In our current study, we show that charge regulation can enable simultaneous coexistence of these two ionized forms within a single homogeneous phase.

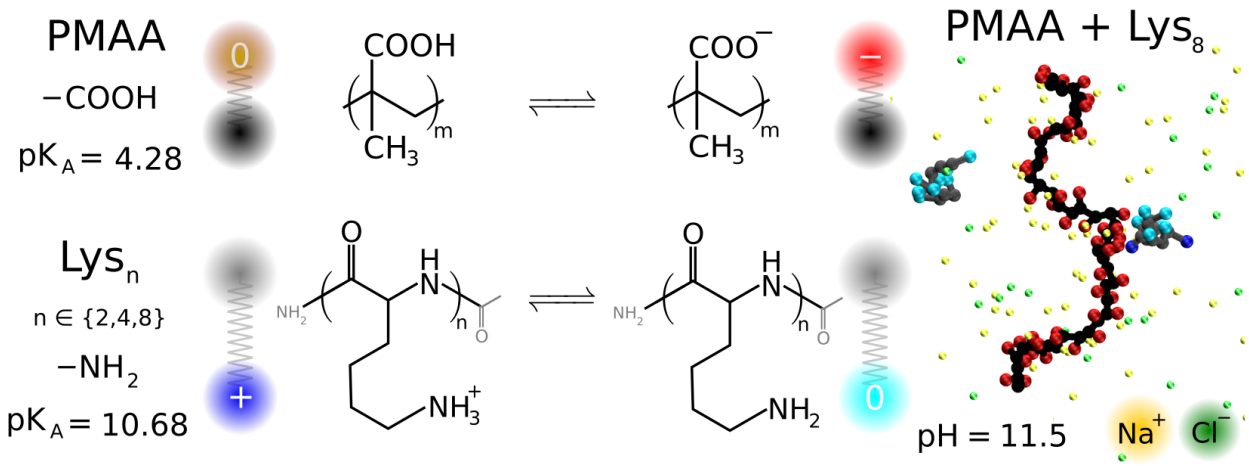

Figure 1: Overview of the investigated system: long anionic poly(methacrylic acid) (PMAA) and short cationic oligolysines (Lys$_n$). The chemical structures on the left show the different ionization states. The schematic next to each chemical structure represents the coarse-grained model that we used for the corresponding chain. Color code: gray and black = backbone groups; orange = non-ionized acidic groups; red = ionized acidic groups; cyan = non-ionized basic groups; blue = ionized basic groups; green = small anion; yellow = small cation.

To demonstrate the significant role of charge regulation, we designed a simple model sys-

tem, consisting of a long polyanion, which has a constant charge in the relevant pH range, and short oligocations which can regulate their charge. Our model polyanion is poly(methacrylic acid), (PMAA, monomer $pK_A \approx 4.28$)[42] and the polycations are oligolysines composed of 2, 4 and 8 lysine residues (ϵ-amino group of the monomer $pK_A = 10.68$),[69] as illustrated in Fig. 1. The molar ratio of lysine to methacrylic monomeric units was 1:2, same as in the experiments. The excess of methacrylic monomers should ensure that even if all lysines condense on the PMAA chains, there is still enough negative charge left on the PMAA to keep the polymer stretched and soluble. Protective groups at the C-end and N-end of each oligolysine ensured that the ionization response was not affected by free carboxyl and amino groups. Using these model molecules, we studied the ionization of oligolysines in aqueous solutions with and without PMAA, demonstrating significant differences between the two. In either case, both oligolysines and PMAA were present at relatively low concentrations in the excess of NaCl, which ensured a fixed ionic strength irrespective of the pH. The pH was adjusted to the desired value by adding extra NaOH or HCl. Full details on the studied system, simulations and experiments are provided in the Methods section and in the electronic supporting information (ESI).

Based on the considerations described above, a significant charge regulation may be expected if the solution pH is close to $pK_A = 10.68$ of the lysine ionizable groups. In the following, we demonstrate using both simulations and experiments, that if the oligolysine polycations are sufficiently long, then they are attracted to the PMAA polyanion at pH values at which the lysines should be uncharged in the absence of the polyanion. At slightly higher pH values, this attraction vanishes, confirming that it is indeed triggered by charge regulation and not by other interactions, such as the hydrogen bonding or hydrophobicity. By comparing oligolysines of various chain lengths, we can further show that indeed electrostatic repulsion between like-charged groups on the lysines suppresses their ionization and shifts their pK_A to lower values, as expected for polybases, and this effect becomes stronger as the chain length increases. On the contrary, their interaction with oppositely charged PMAA

completely reverses this trend, enhancing the ionization and shifting the effective pK_A of oligolysines in the opposite direction. As the lysine chain length is increased, the transition between the non-ionized and fully ionized state becomes more abrupt, in accordance with the strong associative charging numerically predicted by Rathee *et al.*[55] In our simulations and experiments we demonstrate that, if the oligomeric counterion is long enough, then it co-exists in two different states within the same solution: (1) highly charged, condensed on the polyelectrolyte; (2) uncharged, free in solution.

Results and Discussion

Before discussing the interactions between oligolysines and PMAA, it is instructive to discuss the behaviour of free oligolysines in solution, in the absence of PMAA. Fig. 2a shows that the ionization curves of oligolysines are shifted towards lower pH values, as compared to the ideal Henderson-Hasselbalch result, obtained using Equation (1) with $\psi = 0$. This shift increases as the chain length of the oligolysine is increased, reflecting an increase in the electrostatic repulsion between like-charged groups in the oligolysines. The electrostatic repulsion implies an additional free energy cost of the ionization, which causes a diminution in the ionization degree. This shift can be quantified by the effective pK_A value of the side-chains of oligolysines being lower than the corresponding pK_A of the lysine monomer. In addition to the shift in the effective pK_A value, the curves become less steep as the chain length of lysines is increased, in line with previous studies on the titration of various polyacids and polybases in solution.[42,53,70–74]

Fig. 2a also shows that the shifts of the ionization curves of oliglysines may be reversed if these lysines interact with oppositely charged PMAA. In the following, we demonstrate that this enhancement of ionization is caused by electrostatic attraction between the cationic oligolysines and the anionic PMAA. This attraction counter-balances the repulsion between like charges within the lysine molecules, shifting the ionization curves in Fig. 2a towards

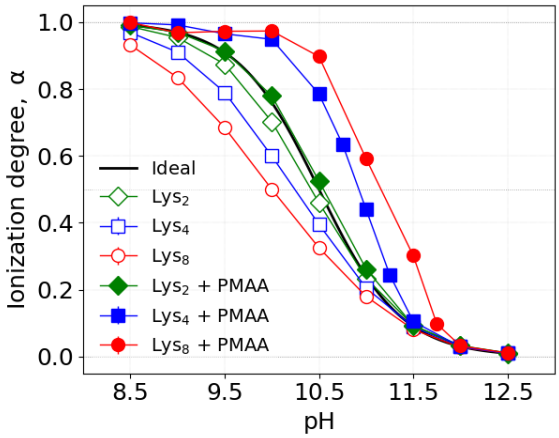

(a) Simulation results for free $\mathrm{Lys_n}$ (empty symbols) and $\mathrm{Lys_n}$ in the presence of PMAA (filled symbols).

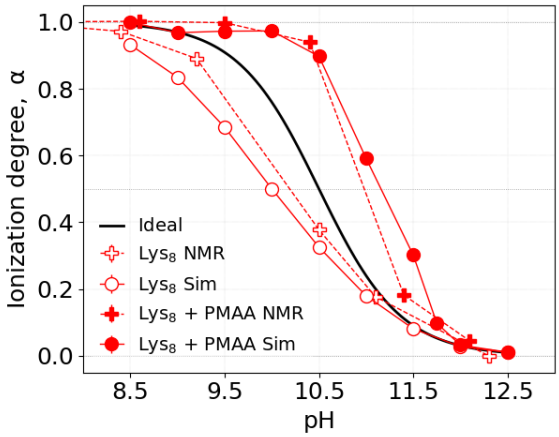

(b) Simulations (circles) and NMR results (crosses) for free $\mathrm{Lys_8}$ (empty symbols) and $\mathrm{Lys_8}$ in presence of PMAA (filled symbols).

Figure 2: Degree of ionization of $\mathrm{Lys_n}$ with $n \in \{2, 4, 8\}$ as a function of pH.

higher pH values (higher effective pK_A). Interestingly, this effect causes that the ionization degree of Lys_2 interacting with PMAA almost perfectly matches the ideal Henderson–Hasselbalch result. Nevertheless, this apparent ideality is caused by mutual compensation of two non-ideal effects. For longer lysines, composed of 4 or 8 units, the ionization curves in Fig. 2a are shifted further to the right of the ideal curve, suggesting that the intramolecular repulsion among the like charges on longer lysines is overcompensated by interaction with the oppositely charged PMAA. In addition, as the chain length of lysines is increased, the ionization curves in the presence of PMAA become increasingly steep, opposite to what we observed for free lysines in the absence of PMAA. By extrapolating this observation to longer chains, one can hypothesize that the transition should approach an infinitely steep first-order transition. In such case, a simultaneous coexistence of fully ionized and non-ionized lysines should be observed within the same system. Later, we show that such coexistence is indeed observed in our simulations. Fig. 2b shows that the ionization degree of Lys_8, experimentally determined from NMR spectra, agrees well with our simulations, both in the presence and in the absence of PMAA. Thus our simulations and experiments confirmed that the interaction with oppositely charged polyelectrolytes can reverse the known effect of electrostatic interactions on the pK_A shift of polyelectrolytes and that the extent of this reversal can be tuned by the chain length.

The anticipated coexistence of lysines in two different states is evidenced in Fig. 3 which shows the populations of oligolysines as a function of their distance to the nearest PMAA monomer, obtained from simulations. These plots show data aggregated over all simulation frames, such that one data point represents one oligolysine observed at a particular distance from the PMMA. To better visualize the populations, a Gaussian scatter has been applied to these points in the vertical direction. In most panels, we observed two clusters of data points: one, within about 1 nm, and another one beyond 10 nm. Notably, first cluster of points is at a distance comparable to the size of a small ion and much smaller than the size of PMAA chain, therefore, it corresponds to condensed oligolysines. On the contrary, the second cluster is at

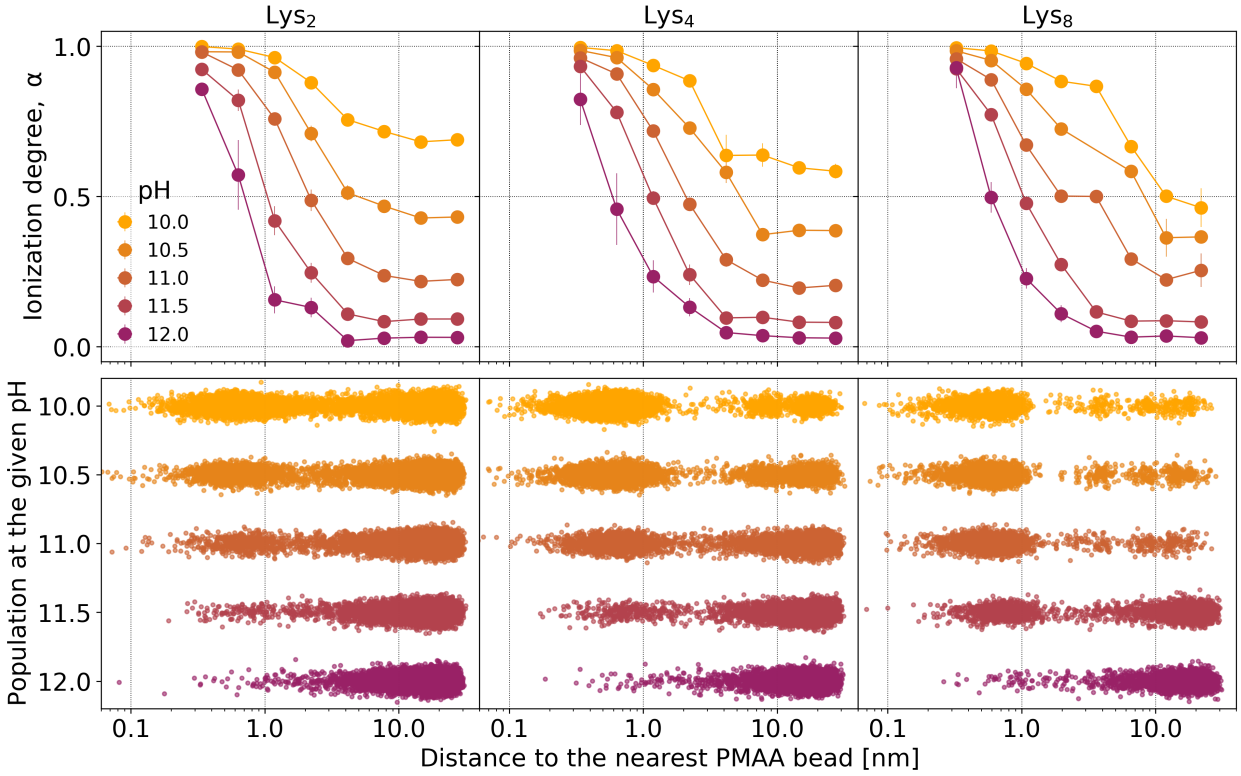

Figure 3: Simulation results for the ionization degree of $\mathrm{Lys_n}$ as a function of distance (top row) and the relative population of lysines as a function of their distance to the nearest bead of the PMAA (bottom row). Each point in the bottom panel corresponds to the distance between the center of mass of one oligolysine molecule and the closest PMAA bead in each of the simulation frames.

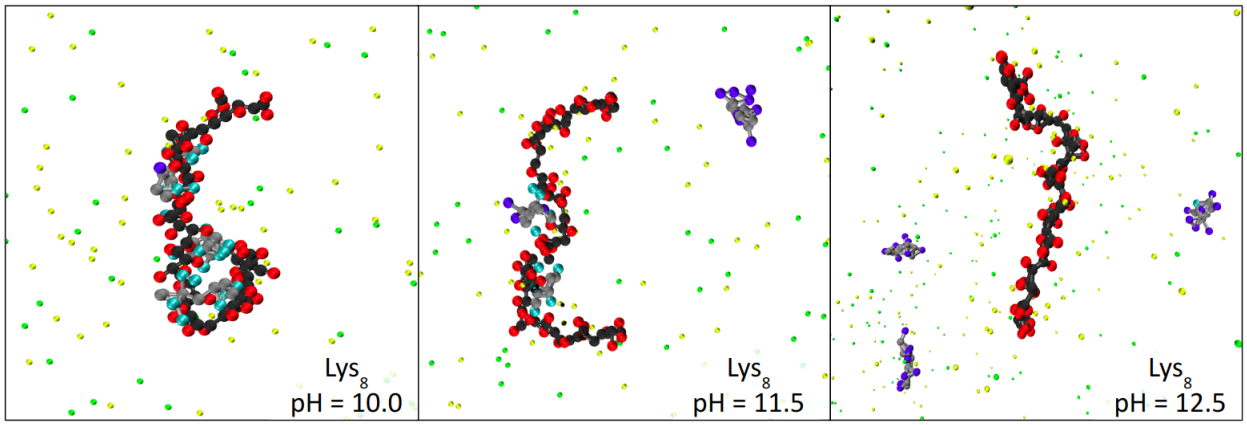

Figure 4: Simulation snapshots of the $\mathrm{Lys_8}$ interacting with PMAA. At pH = 10.0 ($\lesssim \mathrm{p}K_\mathrm{A}^\mathrm{eff}$) the lysines are highly ionized and condensed on the PMAA chain, at pH = 12.5 ($\gtrsim \mathrm{p}K_\mathrm{A}^\mathrm{eff}$) the lysines are weakly ionized and free in solution. However, at pH = 11.5 ($\approx \mathrm{p}K_\mathrm{A}^\mathrm{eff}$) the two different ionization states coexist in the solution. Color code is the same as in Fig. 1.

a distance greater than the size of PMAA, therefore, it corresponds to free lysines. As an alternative representation, we plot the same data aggregated into a histogram in Fig. S1. As evidenced by the plots of ionization degree as a function of distance in Fig. 3, the condensed oligolysines are highly ionized whereas those far from the polyelectrolyte are practically non-ionized. This local variation of the degree of ionization of lysines well correlates with the local variation in the local concentration of H^+ ions as a function of distance from the PMAA monomers, shown in Fig. S2. Indeed, we observe an increase in the local concentration of H^+ ions nearby the PMAA chain that could alternatively explain the increase in the degree of ionization of Lys. The local concentration of H^+ ions, sometimes incorrectly termed the "local pH",[52,73] reflects the local variation of the electrostatic potential, which determines the excess contribution to the free energy of dissociation of the titratable groups on oligolysines. Fig. S2 demonstrates that the "local pH" at the PMAA chain is slightly lower for Lys_2 than Lys_4 and Lys_8, which correlates with slightly lower ionization of Lys_2 at the PMAA chain. On the other hand, at pH = 12, the "local pH" is around 10.5 or higher, suggesting that the lysines should not be fully ionized when condensed on the PMAA chain(cf. Fig. 2). However, Fig. 3 shows that, even at the highest pH values, all lysines are almost fully ionized when condensed on the PMAA, indicating an additional contribution which cannot be explanined solely by the "local pH" effects.

As the pH is increased, the number of highly ionized lysines close to the polyelectrolyte decreases and consistently the number of non-ionized lysines far from the polyelectrolyte increases. For Lys_2, we observe that the population of highly ionized lysines practically vanishes at pH > 10.5 whereas for longer lysines this population persists up to much higher pH values. Furthermore, the populations of highly charged and uncharged lysines are much more clearly separated for longer lysine chains whereas the shorter lysines are more likely to be found at intermediate distances and intermediate ionization degrees. Within the counterion condensation framework, this effect could be interpreted so that the highly ionized lysines condense on the PMAA chain whereas the weakly ionized ones do not condense.

The same effect could be interpreted within the charge regulation framework, so that the lysines increase their charge to enable their condensation on the chain. In practice, both charge regulation and condensation occur simultaneously, causing that longer lysines exist within the same system in two distinct states: either highly charged and condensed on the polyelectrolyte or uncharged and free in solution (non-condensed) as can be observed in the simulation snapshots of the system with Lys_8 in Fig. 4. The simulation snapshots of the systems with Lys_2 and Lys_4 are shown in Fig. S5.

To quantify the condensation of lysines on the PMAA chain, we computed the fraction of free lysines at various pH values, shown in Fig. 5a. We considered the lysines to be condensed if they were closer to the PMAA chain than 2 nm. We chose this threshold because it approximately corresponds to the local minimum in the populations of lysines as a function of distance to the neareast PMAA bead, shown in Fig. 3. Fig. 5a shows that at pH $\lesssim$ 10 about 30-40% of the shorter lysines (Lys_2) condense on the PMAA chain whereas the remaining 60-70% are free in solution. In contrast, about 90% of the longer lysines (Lys_4 and Lys_8) condense on PMAA under the same conditions. This is expected because the longer lysines bear a higher charge when fully ionized, therefore, they condense more strongly. As the pH is increased, the fraction of condensed Lys_2 gradually decreases and approaches zero at pH $\approx$ 11.5. The fraction of condensed Lys_4 remains high up to a higher pH and then decreases more abruptly, as compared to Lys_2. Finally, the Lys_8 exhibit a rather sharp transition between completely condensed and completely free state within about 0.5 units of pH, resembling a first-order phase transition.

The condensation of lysines at various pH values is further reflected by changes in the PMAA conformation, as evidenced by the plot of its end-to-end distance as a function of pH in Fig. 5b. In all cases, the condensed lysines cause a shrinkage of the PMAA chain. As the pH is increased, the end-to-end distance of PMAA increases, reaching the same saturation value at a high pH, as the lysines gradually lose their charge and detach from the PMAA chain. Therefore, this increase in end-to-end distance very well correlates with the

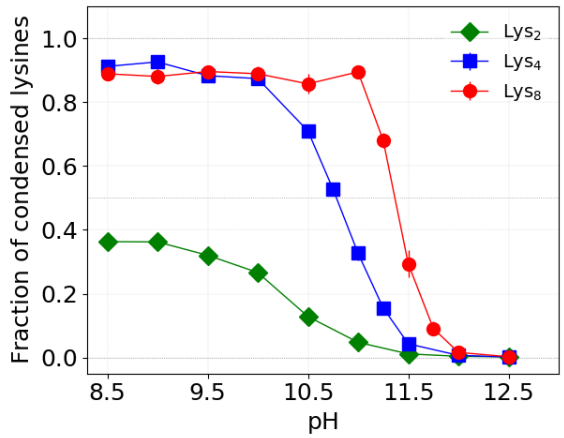

(a) Fraction of Lys_n condensed on the PMAA, obtained from simulations.

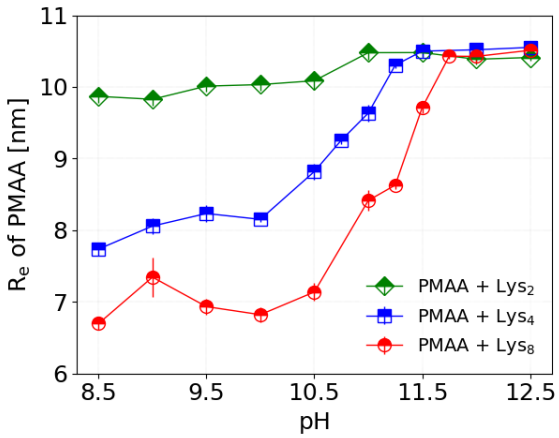

(b) End-to-end distance of PMAA in presence of Lys_n, obtained from simulations.

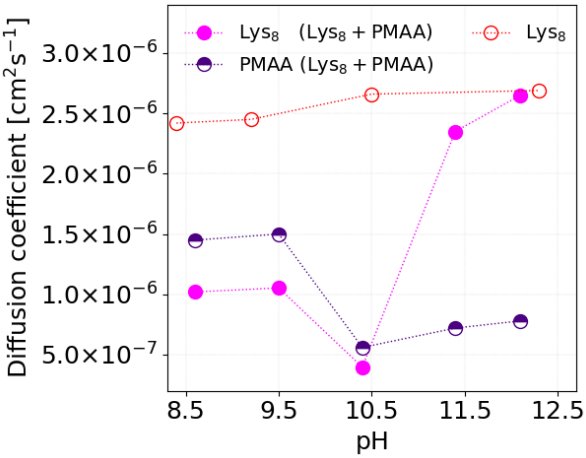

(c) Diffusion coefficient of Lys_8 and PMAA in a common solution (labeled as Lys_8+PMAA), compared to free Lys_8 in the absence of PMAA, determined from DOSY NMR experiments.

Figure 5: Condensation, swelling of the PMAA for Lys_n with $n \in \{2, 4, 8\}$ and diffusion of Lys_8 in presence and absence of PMAA as a function of pH.

decrease of the fraction of condensed lysines (Fig. 5a) and concomitantly it correlates with the decrease in their degree of ionization (Fig. 2a). The condensation of Lys_2 has a much smaller effect on the end-to-end distance than Lys_4 or Lys_8. The difference between Lys_2 and Lys_4 could be explained by the lower fraction of condensed Lys_2. However, the same argument cannot explain the difference between Lys_4 and Lys_8 at low pH because they are both fully ionized and condense to the same extent at pH $\lesssim$ 10. Therefore, the difference in the end-to-end distance of PMAA interacting with Lys_4 and Lys_8 demonstrates that there is an additional cooperativity between the ionization and condensation for longer lysines, whereas this cooperativity is very weak for short lysines.

Finally, Fig. 5c shows the diffusion coefficients of Lys_8 and PMAA, determined from DOSY NMR measurements at various pH values. Expectedly, the diffusion coefficient of free Lys_8 in solution in the absence of PMAA is only weakly affected by the pH. On the contrary, the diffusion coefficient of Lys_8 in the presence of PMAA strongly depends on the pH. At low pH, when the lysine is charged and condensed on the PMAA chain, the diffusion coefficients of Lys_8 and PMAA are very similar and significantly lower than the diffusion coefficient of lysine without PMAA. As the pH is increased, the diffusion coefficient of Lys_8 abruptly increases, attaining the same value as the diffusion coefficient of lysine in the solution without PMAA. An independent piece of evidence of the interaction between PMAA and Lysines is provided by the cross peak between PMAA and Lys_8 in NOESY NMR spectra, shown in Fig. S15. This peak is present at pH $\leq$ 10.4, indicating that PMAA and Lys_8 interact at lower pH values, but it vanishes at pH $\geq$ 11.4, indicating that they no longer interact at the higher pH values. Therefore, we can conclude that not only simulations but also experiments indicate that the long lysines condense on the PMAA chain at pH $\lesssim$ 10.4 whereas they remain free at pH $\gtrsim$ 11.4.

Conclusions

Using a model system, composed of long anionic poly(methacrylic acid) (PMAA) and short polycationic oligolysines, we demonstrated how charge regulation affects interactions between two oppositely charged macromolecules. From both experiments and simulations we observed that the net charge of free oligolysines in the absence of PMAA is lower than that of the parent monomer, which can be quantified by a shift in their effective pK_A values. This shift is stronger for longer oligolysines, in accordance with the established knowledge in the field of polyelectrolytes. However, if these oligolysines interact with the anionic PMAA, they condense on the polyanion. This condensation is accompanied by an increase in the net charge of the oligolysines. Ultimately, this increase in the ionization reverses the pK_A shifts of lysines, causing that the effective pK_A is higher than that of the parent monomer. The latter effect is enhanced as the length of the lysines is increased. Furthermore, our simulations have shown that the longer oligolysines simultaneously exists in two different ionization states within the same system: one highly ionized and condensed and another one practically non-ionized and free in solution. Notably, individual lysine oligomers dynamically are dynamically exchanged between the condensed and free states. The correlation between condensation and ionization was further confirmed by our NMR experiments. The transition between these two states as a function of pH becomes sharper as the chain length of oligolysine is increased, resembling a first-order transition. If we extrapolate our findings to longer chains, they suggest that charge regulation should play a significant role in interactions between oppositely charged macromolecules, enhancing their ionization and thereby enabling association at pH values where one or both macromolecules should be uncharged in the absence of the oppositely charged polymeric partner. This effect should be particularly important if the solution pH is not far from the pK_A of one or both macromolecules. The effect is not unique to peptides interacting with polyelectrolytes but should apply to any oligomeric counterions if the solution pH is close to their pK_A value.

The simplicity of both the experimental setup and the coarse-grained simulation model

underscores the universality of our results. The prospect of tailoring the complexation by engineering the charge regulation is relevant mainly for materials design and biomedical applications. For example, complexation of small cationic pro-inflammatory cytokines such as cathelicidin with polyanions, such as extracellular DNA, is crucial for the defence of the organism against bacteria[75] and also for development of autoimmune diseases.[76] Likewise, anionic polysaccharide heparin, clinically used as a coagulant, can be neutralized with positively charged peptide protamin.[77,78] The heparine-protamin complexation can be observed also at pH $\approx$ 7.4 corresponding to the blood conditions, where protamin should be only weakly charged. At the same time, low molecular weight (fractionated) heparin exhibits weaker complexation with protamin,[79] which can be explained by the mechanisms described by our study. The fundamental understanding of the interplay of oligocation length and charge regulation presented above can guide design of heparin sensors[80] or development of alternative antidotes. Similarly, the mechanisms revealed in our study can explain why gels fromed by charged cellulose nanocrystals and poly(allylamine) remain ionized and stable over a broader pH range than could be expected from their solution behaviour.[81] The extrapolation of our results from short peptides and charged oligomers also to complex molecules such as proteins containing lysine-rich or carboxylate-rich sequences is in principle possible. Nevertheless, it is known that in such complex environments hydrogen bonding[82–84] and other interactions can become as important as electrostatics. For such systems, quantitative simulations with predictive power would require refinement of our models, by including the hydrogen bonds, as is currently underway.

Methods

Simulation model and method

To gain detailed insights into charge regulation in the PMAA-lysine system, we employed computer simulations using a coarse-grained bead-spring model in implicit solvent with ex-

plicit ions. In our model, each monomeric unit was represented by two spherical beads, one representing the polymer backbone and the other one representing the side chain, as illustrated in Fig. 1. Parameters of this model were set using semi-empirical estimates based our previous studies.[44,61,85,86]

The PMAA consisted of 48 monomeric units and the oligolysines consisted of $n \in \{2, 4, 8\}$ units, denoted as $\mathrm{Lys_n}$. The number of Lysine oligomers was chosen such that the molar ratio of lysine monomeric units to PMAA was 1:2, same as in the experiments. The C-end and the N-end were not charged in our model of oligolysines because it was designed to represent the oligopeptides used in our experiments, which had both ends protected by non-ionizable groups. In addition to PMAA and oligolysines, small ions ($\mathrm{Na^+}$, $\mathrm{Cl^-}$) were present in the system to ensure ionic strength $I = 0.01\,\mathrm{M}$. We assumed that PMAA side chains were fully ionized because we were interested only in $\mathrm{pH} > 8$ which is much greater than $\mathrm{p}K_\mathrm{A}^\mathrm{PMAA}$, so PMAA should be fully ionized. By contrast, the ionization states of lysine side chains were allowed to fluctuate.

The chain length of PMAA in simulations, $m = 48$, was chosen such as to make it much longer than all lysine oligomers, yet not too long to enable efficient sampling of the configuration space in simulations. Our previous studies of similar models suggested that the ionization and local conformational properties of polyelectrolytes do not change much at chain lengths $m \gtrsim 50$.[73] We chose $m = 48$ because it is divisible by $n \in \{2, 4, 8\}$, so that all simulations could be performed at 1:2 molar ratio of lysine to methacrylate monomeric units. Based on the above considerations, simulated PMAA chains were much shorter than $m \approx 1150$ used in our experiments, this difference should not significantly affect our observations and conclusions. To support this claim, we ran a set of simulations of PMAA with $m = 96$ and $\mathrm{Lys_n}$ at selected pH values at the same molar ratio and concentrations as our original simulations. These simulations, provided in the ESI, section 1.5, show that doubling of the PMAA chain length has no significant effect on the interpretation of the results.

The molar ratio of lysine to methacrylic units 1:2 was chosen based on earlier simulations performed in the master thesis of Roman Staňo.[60] In this thesis, he showed that at higher molar ratios the oligopeptides condense on the polyanion to such an extent, that they almost fully compensate its charge. This causes significant compaction of the chain, which should cause precipitation in an experimental system. The precipitation is undesired because the polymer and peptide content in the precipitate might be different from the bulk solution. Simultaneously, a high peptide content is desired to ensure favourable signal-to-noise ratio when its behavior both in simulations and experiments. Thus, our choice of 1:2 lysine to methacrylate molar ratio was chosen as a compromise between these two competing requirements.

We sampled the ionization states of lysine side chains using the constant-pH method,[87] with $\mathrm{p}K_{\mathrm{A}}^{\mathrm{lys}} = 10.68$ as the input parameter. This method entails a Monte Carlo (MC) procedure, in which the ionization state is changed from protonated to deprotonated or vice versa, while simultaneously inserting or deleting a counterion in order to keep the simulation box electroneutral, represented by a schematic chemical reaction

$$\mathrm{BH}^{+} \rightleftharpoons \mathrm{B}^{0} + \mathrm{H}^{+}. \tag{2}$$

The acceptance probability of the MC trial move is given by[87]

$$P_{\mathrm{cpH}} = \min\left[1, \exp\left(-\frac{\Delta U}{\mathrm{k_B}T} + \xi \ln(10)\left(\mathrm{pH} - \mathrm{p}K_{\mathrm{a}}\right)\right)\right], \tag{3}$$

where ΔU is the change in potential energy, $\xi = 1$ if the base group is being deprotonated and $\xi = -1$ if it is being deprotonated in the reaction given by Eq. 2. The MC moves for sampling the ionization states were coupled to sampling of the configuration space by Langevin Dynamics. The degree of ionization is then computed as an ensemble average over the ionization states in different configurations sampled during the simulation. All simulations were performed using the software ESPResSo v4.1.4.[88,89] Full details on the

simulation model, simulation protocol and data processing are provided in the ESI.

Experimental

To complement the simulations, we studied experimentally the ionization of oligolysines and their interactions with poly(methacrylic acid) using potentiometric titrations and nuclear magnetic resonance (NMR). The simulated PMAA chains consisted of $m \approx 1150$ monomeric units, estimated from the average molar mass. The $\mathrm{Lys_n}$ samples with $n \in \{2, 4, 8\}$ were custom-synthesized at high purity. The C- end of each oligolysine was protected by a primary amide $-\mathrm{CONH_2}$ and the N- end was protected by an acetamido group $-\mathrm{NHCOCH_3}$ in order to ensure that the ionization response was not affected by free carboxyl and amino groups. From the potentiometric titrations we determined the net charge of oligolysines as a function of the pH, which enabled us to validate the simulation model. From NMR chemical shifts, we determined the degree of ionization of oligolysines in solutions with and without PMAA, demonstrating significant differences between the two. Additionally, we used NMR to determine the diffusion coefficients of PMAA and oligolysines, which allowed us to determine if the two molecules diffuse independently or not. Full details on the experiments and data analysis are provided in the ESI.

Acknowledgement

P.K., P.M.B., P.M. and M.Š. acknowledge financial support of the Czech Science foundation, grant 21-31978J. R.S. acknowledges the financial support by the Doctoral College Advanced Functional Materials – Hierarchical Design of Hybrid Systems DOC 85 doc.funds funded by the Austrian Science Fund (FWF). P.M.B. also acknowledges the financial support from the Spanish Ministry of Universities (Margarita Salas Grant MS98), from the Generalitat de Catalunya (Grant 2021SGR00350) and from the European Union's Horizon Europe research and innovation programme under the Marie Sklodowska-Curie grant agreement No

101062456 (ModEMUS). P.M.B. and P.K. acknowledge the funding from the Norway grants, provided by the Czech Ministry of finance, project number EHP-BFNU-OVNKM-4-215-01-2022. M.H. and J.P. Thank to the Ministry of Education, Youth and Sports of the Czech Republic, grant # EATRIS CZ - LM2023053. M.Š. acknowledges the support by the Operational Programme Research, Development and Education: "Excellent Research Teams" (Project No. CZ.02.1.01/0.0/0.0/15_003/0000417-CUCAM). Computational resources were supplied by the project "e-Infrastruktura CZ" (e-INFRA CZ LM2018140) supported by the Ministry of Education, Youth and Sports of the Czech Republic.

Supporting Information Available

Experimental procedures, details on simulation methods and additional results.

References

(1) Schiessel, H. The physics of chromatin. *Journal of Physics: Condensed Matter* **2003**, *15*, R699.

(2) Korolev, N.; Vorontsova, O. V.; Nordenskiöld, L. Physicochemical analysis of electrostatic foundation for DNA–protein interactions in chromatin transformations. *Progress in Biophysics and Molecular Biology* **2007**, *95*, 23–49.

(3) Belyi, V. A.; Muthukumar, M. Electrostatic origin of the genome packing in viruses. *Proceedings of the National Academy of Sciences* **2006**, *103*, 17174–17178.

(4) Borukhov, I.; Bruinsma, R. F.; Gelbart, W. M.; Liu, A. J. Structural polymorphism of the cytoskeleton: A model of linker-assisted filament aggregation. *Proceedings of the National Academy of Sciences* **2005**, *102*, 3673–3678.

(5) Sing, C. E.; Perry, S. L. Recent progress in the science of complex coacervation. *Soft Matter* **2020**, *16*, 2885–2914.

(6) van der Gucht, J.; Spruijt, E.; Lemmers, M.; Cohen Stuart, M. A. Polyelectrolyte complexes: Bulk phases and colloidal systems. *Journal of Colloid and Interface Science* **2011**, *361*, 407–422.

(7) Banani, S. F.; Lee, H. O.; Hyman, A. A.; Rosen, M. K. Biomolecular condensates: organizers of cellular biochemistry. *Nature Reviews Molecular Cell Biology* **2017**, *18*, 285–298.

(8) Dobrynin, A. V.; Rubinstein, M. Theory of polyelectrolytes in solutions and at surfaces. *Progress in Polymer Science* **2005**, *30*, 1049–1118.

(9) Muthukumar, M. 50*th* Anniversary Perspective: A Perspective on Polyelectrolyte Solutions. *Macromolecules* **2017**, *50*, 9528–9560.

(10) Levin, Y. Electrostatic correlations: from plasma to biology. *Reports on Progress in Physics* **2002**, *65*, 1577.

(11) Hueckel, T.; Hocky, G. M.; Palacci, J.; Sacanna, S. Ionic solids from common colloids. *Nature* **2020**, *580*, 487–490.

(12) Bianchi, E.; Kahl, G.; Likos, C. N. Inverse patchy colloids: from microscopic description to mesoscopic coarse-graining. *Soft Matter* **2011**, *7*, 8313–8323.

(13) Otter, R.; Besenius, P. Supramolecular assembly of functional peptide–polymer conjugates. *Organic & Biomolecular Chemistry* **2019**, *17*, 6719–6734.

(14) Frisch, H.; Unsleber, J. P.; Lüdeker, D.; Peterlechner, M.; Brunklaus, G.; Waller, M.; Besenius, P. pH-Switchable Ampholytic Supramolecular Copolymers. *Angewandte Chemie International Edition* **2013**, *52*, 10097–10101.

(15) Chan, K. H.; Lee, W. H.; Zhuo, S.; Ni, M. Harnessing supramolecular peptide nanotechnology in biomedical applications. *International Journal of Nanomedicine* **2017**, *Volume 12*, 1171–1182.

(16) Aggeli, A.; Bell, M.; Boden, N.; Carrick, L. M.; Strong, A. E. Self-Assembling Peptide Polyelectrolyte β-Sheet Complexes Form Nematic Hydrogels. *Angewandte Chemie International Edition* **2003**, *42*, 5603–5606.

(17) Briggs, B. D.; Knecht, M. R. Nanotechnology Meets Biology: Peptide-based Methods for the Fabrication of Functional Materials. *The Journal of Physical Chemistry Letters* **2012**, *3*, 405–418.

(18) Yeung, C. L.; Iqbal, P.; Allan, M.; Lashkor, M.; Preece, J. A.; Mendes, P. M. Tuning Specific Biomolecular Interactions Using Electro-Switchable Oligopeptide Surfaces. *Advanced Functional Materials* **2010**, *20*, 2657–2663.

(19) Kichler, A. Gene transfer with modified polyethylenimines. *The Journal of Gene Medicine* **2004**, *6*, S3–S10.

(20) Boussif, O.; Lezoualc'h, F.; Zanta, M. A.; Mergny, M. D.; Scherman, D.; Demeneix, B.; Behr, J. P. A versatile vector for gene and oligonucleotide transfer into cells in culture and in vivo: polyethylenimine. *Proceedings of the National Academy of Sciences* **1995**, *92*, 7297–7301.

(21) Gill, A.; Scanlon, T. C.; Osipovitch, D. C.; Madden, D. R.; Griswold, K. E. Crystal Structure of a Charge Engineered Human Lysozyme Having Enhanced Bactericidal Activity. *PLOS ONE* **2011**, *6*, 1–7.

(22) Nie, C.; Sahoo, A. K.; Netz, R. R.; Herrmann, A.; Ballauff, M.; Haag, R. Charge Matters: Mutations in Omicron Variant Favor Binding to Cells. *ChemBioChem* **2022**, *23*, e202100681.

(23) Partridge, L. J.; Urwin, L.; Nicklin, M. J. H.; James, D. C.; Green, L. R.; Monk, P. N. ACE2-Independent Interaction of SARS-CoV-2 Spike Protein with Human Epithelial Cells Is Inhibited by Unfractionated Heparin. *Cells* **2021**, *10*, 1419.

(24) Suryawanshi, R.; Patil, C.; Koganti, R.; Singh, S.; Ames, J.; Shukla, D. Heparan Sulfate Binding Cationic Peptides Restrict SARS-CoV-2 Entry. *Pathogens* **2021**, *10*, 803.

(25) Manning, G. S. Limiting Laws and Counterion Condensation in Polyelectrolyte Solutions I. Colligative Properties. *The Journal of Chemical Physics* **1969**, *51*, 924–933.

(26) Oosawa, F. A simple theory of thermodynamic properties of polyelectrolyte solutions. *Journal of Polymer Science* **1957**, *23*, 421–430.

(27) Naji, A.; Netz, R. R. Scaling and universality in the counterion-condensation transition at charged cylinders. *Phys. Rev. E* **2006**, *73*, 056105.

(28) Muthukumar, M. Theory of counter-ion condensation on flexible polyelectrolytes: Adsorption mechanism. *The Journal of Chemical Physics* **2004**, *120*, 9343–9350.

(29) Raspaud, E.; Da Conceicao, M.; Livolant, F. Do free DNA counterions control the osmotic pressure? *Physical Review Letters* **2000**, *84*, 2533.

(30) Heyda, J.; Dzubiella, J. Ion-specific counterion condensation on charged peptides: Poisson–Boltzmann vs. atomistic simulations. *Soft Matter* **2012**, *8*, 9338–9344.

(31) Smiatek, J. Theoretical and Computational Insight into Solvent and Specific Ion Effects for Polyelectrolytes: The Importance of Local Molecular Interactions. *Molecules* **2020**, *25*, 1661.

(32) Henzler, K.; Haupt, B.; Lauterbach, K.; Wittemann, A.; Borisov, O.; Ballauff, M. Adsorption of β-actoglobulin on spherical polyelectrolyte brushes: Direct proof of counterion release by isothermal titration calorimetry. *Journal of the American Chemical Society* **2010**, *132*, 3159–3163.

(33) Ran, Q.; Xu, X.; Dzubiella, J.; Haag, R.; Ballauff, M. Thermodynamics of the Binding of Lysozyme to a Dendritic Polyelectrolyte: Electrostatics Versus Hydration. *ACS Omega* **2018**, *3*, 9086–9095, PMID: 31459043.

(34) Xu, X.; Ran, Q.; Dey, P.; Nikam, R.; Haag, R.; Ballauff, M.; Dzubiella, J. Counterion-Release Entropy Governs the Inhibition of Serum Proteins by Polyelectrolyte Drugs. *Biomacromolecules* **2018**, *19*, 409–416.

(35) Chen, S.; Wang, Z.-G. Driving force and pathway in polyelectrolyte complex coacervation. *Proceedings of the National Academy of Sciences* **2022**, *119*, e2209975119.

(36) Fu, J.; Schlenoff, J. B. Driving Forces for Oppositely Charged Polyion Association in Aqueous Solutions: Enthalpic, Entropic, but Not Electrostatic. *Journal of the American Chemical Society* **2016**, *138*, 980–990, PMID: 26771205.

(37) Ziebarth, J. D.; Wang, Y. Understanding the protonation behavior of linear polyethylenimine in solutions through Monte Carlo simulations. *Biomacromolecules* **2010**, *11*, 29–38.

(38) Ziebarth, J.; Wang, Y. Molecular Dynamics Simulations of DNA-Polycation Complex Formation. *Biophysical Journal* **2009**, *97*, 1971–1983.

(39) Bloomfield, V. A. Condensation of DNA by multivalent cations: Considerations on mechanism. *Biopolymers* **1991**, *31*, 1471–1481.

(40) Priftis, D.; Laugel, N.; Tirrell, M. Thermodynamic Characterization of Polypeptide Complex Coacervation. *Langmuir* **2012**, *28*, 15947–15957, PMID: 23083137.

(41) Ou, Z.; Muthukumar, M. Entropy and enthalpy of polyelectrolyte complexation: Langevin dynamics simulations. *The Journal of Chemical Physics* **2006**, *124*, 154902.

(42) Arnold, R. The titration of polymeric acids. *Journal of Colloid Science* **1957**, *12*, 549–556.

(43) Koper, G. J. M.; Van Duijvenbode, R. C.; Stam, D. D. P. W.; Steuerle, U.; Borkovec, M. Synthesis and Protonation Behavior of Comblike Poly(ethyleneimine). *Macromolecules* **2003**, *36*, 2500–2507.

(44) Lunkad, R.; Biehl, P.; Murmiliuk, A.; Blanco, P. M.; Mons, P.; Štěpánek, M.; Schacher, F. H.; Košovan, P. Simulations and Potentiometric Titrations Enable Reliable Determination of Effective pK_a Values of Various Polyzwitterions. *Macromolecules* **2022**, *55*, 7775–7784.

(45) Blanco, P. M.; Achetoni, M. M.; Garcés, J. L.; Madurga, S.; Mas, F.; Baieli, M. F.; Narambuena, C. F. Adsorption of flexible proteins in the 'wrong side' of the isoelectric point: Casein macropeptide as a model system. *Colloids and Surfaces B: Biointerfaces* **2022**, *217*, 112617.

(46) Blanco, P. M.; Narambuena, C. F.; Madurga, S.; Mas, F.; Garcés, J. L. Unusual Aspects of Charge Regulation in Flexible Weak Polyelectrolytes. *Polymers* **2023**, *15*, 2680.

(47) Lund, M.; Jönsson, B. Charge regulation in biomolecular solution. *Quarterly reviews of biophysics* **2013**, *46*, 265–281.

(48) Narayanan Nair, A. K.; Uyaver, S.; Sun, S. Conformational transitions of a weak polyampholyte. *The Journal of Chemical Physics* **2014**, *141*, 134905.

(49) Ulrich, S.; Seijo, M.; Stoll, S. A Monte Carlo Study of Weak Polyampholytes: Stiffness and Primary Structure Influences on Titration Curves and Chain Conformations. *The Journal of Physical Chemistry B* **2007**, *111*, 8459–8467.

(50) Ulrich, S.; Seijo, M.; Carnal, F.; Stoll, S. Formation of Complexes between Nanoparticles and Weak Polyampholyte Chains. Monte Carlo Simulations. *Macromolecules* **2011**, *44*, 1661–1670.

(51) Barroso da Silva, F. L.; Boström, M.; Persson, C. Effect of Charge Regulation and Ion–Dipole Interactions on the Selectivity of Protein–Nanoparticle Binding. *Langmuir* **2014**, *30*, 4078–4083.

(52) Murmiliuk, A.; Košovan, P.; Janata, M.; Procházka, K.; Uhlík, F.; Štěpánek, M. Local pH and Effective pK of a Polyelectrolyte Chain: Two Names for One Quantity? *ACS Macro Letters* **2018**, *7*, 1243–1247.

(53) Landsgesell, J.; Nová, L.; Rud, O.; Uhlík, F.; Sean, D.; Hebbeker, P.; Holm, C.; Košovan, P. Simulations of ionization equilibria in weak polyelectrolyte solutions and gels. *Soft Matter* **2019**, *15*, 1155–1185.

(54) Košovan, P.; Landsgesell, J.; Nová, L.; Uhlík, F.; Beyer, D.; Blanco, P. M.; Staňo, R.; Holm, C. Reply to the 'Comment on "Simulations of ionization equilibria in weak polyelectrolyte solutions and gels"' by J. Landsgesell, L. Nová, O. Rud, F. Uhlík, D. Sean, P. Hebbeker, C. Holm and P. Košovan, Soft Matter, 2019, 15, 1155–1185. *Soft Matter* **2023**, *19*, 3522–3525.

(55) Rathee, V. S.; Sidky, H.; Sikora, B. J.; Whitmer, J. K. Role of Associative Charging in the Entropy–Energy Balance of Polyelectrolyte Complexes. *Journal of the American Chemical Society* **2018**, *140*, 15319–15328.

(56) Staňo, R.; Košovan, P.; Tagliabue, A.; Holm, C. Electrostatically Cross-Linked Reversible Gels—Effects of pH and Ionic Strength. *Macromolecules* **2021**, *54*, 4769–4781.

(57) Voets, I. K.; De Keizer, A.; Cohen Stuart, M. A. Complex coacervate core micelles. *Advances in Colloid and Interface Science* **2009**, *147-148*, 300–318.

(58) Krogstad, D. V.; Lynd, N. A.; Choi, S.-H.; Spruell, J. M.; Hawker, C. J.; Kramer, E. J.; Tirrell, M. V. Effects of Polymer and Salt Concentration on the Structure and Properties of Triblock Copolymer Coacervate Hydrogels. *Macromolecules* **2013**, *46*, 1512–1518.

(59) Albertazzi, L.; Martinez-Veracoechea, F. J.; Leenders, C. M. A.; Voets, I. K.; Frenkel, D.; Meijer, E. W. Spatiotemporal control and superselectivity in supramolecular polymers using multivalency. *Proceedings of the National Academy of Sciences* **2013**, *110*, 12203–12208.

(60) Staňo Roman, R. Effect of acid-base equilibria on the association behaviour of polyelectrolytes. M.Sc. thesis, Charles University, Prague, 2020.

(61) Lunkad, R.; Barroso da Silva, F. L.; Košovan, P. Both Charge-Regulation and Charge-Patch Distribution Can Drive Adsorption on the Wrong Side of the Isoelectric Point. *Journal of the American Chemical Society* **2022**, *144*, 1813–1825.

(62) Achazi, K.; Haag, R.; Ballauff, M.; Dernedde, J.; Kizhakkedathu, J. N.; Maysinger, D.; Multhaup, G. Understanding the Interaction of Polyelectrolyte Architectures with Proteins and Biosystems. *Angewandte Chemie International Edition* **2021**, *60*, 3882–3904.

(63) Choi, S.; Knoerdel, A. R.; Sing, C. E.; Keating, C. D. Effect of Polypeptide Complex Coacervate Microenvironment on Protonation of a Guest Molecule. *The Journal of Physical Chemistry B* **2023**, *127*, 5978–5991, PMID: 37350455.

(64) Digby, Z. A.; Yang, M.; Lteif, S.; Schlenoff, J. B. Salt Resistance as a Measure of the Strength of Polyelectrolyte Complexation. *Macromolecules* **2022**, *55*, 978–988.

(65) Choi, J.; Rubner, M. F. Influence of the Degree of Ionization on Weak Polyelectrolyte Multilayer Assembly. *Macromolecules* **2005**, *38*, 116–124.

(66) Petrov, A. I.; Antipov, A. A.; Sukhorukov, G. B. Base-Acid Equilibria in Polyelectrolyte Systems: From Weak Polyelectrolytes to Interpolyelectrolyte Complexes and Multilayered Polyelectrolyte Shells. *Macromolecules* **2003**, *36*, 10079–10086.

(67) Knoerdel, A. R.; Blocher McTigue, W. C.; Sing, C. E. Transfer Matrix Model of pH Ef-

fects in Polymeric Complex Coacervation. *The Journal of Physical Chemistry B* **2021**, *125*, 8965–8980, PMID: 34328340.

(68) Salehi, A.; Larson, R. G. A Molecular Thermodynamic Model of Complexation in Mixtures of Oppositely Charged Polyelectrolytes with Explicit Account of Charge Association/Dissociation. *Macromolecules* **2016**, *49*, 9706–9719.

(69) Haynes, W. *CRC Handbook of Chemistry and Physics*, 96th ed.; CRC Press: New York, 2015.

(70) Panagiotopoulos, A. Charge correlation effects on ionization of weak polyelectrolytes. *Journal of Physics: Condensed Matter* **2009**, *21*, 424113.

(71) Borukhov, I.; Andelman, D.; Borrega, R.; Cloitre, M.; Leibler, L.; Orland, H. Polyelectrolyte Titration: Theory and Experiment. *The Journal of Physical Chemistry B* **2000**, *104*, 11027–11034.

(72) Garcés, J.; Madurga, S.; Borkovec, M. Coupling of conformational and ionization equilibria in linear poly (ethylenimine): A study based on the site binding/rotational isomeric state (SBRIS) model. *Physical Chemistry Chemical Physics* **2014**, *16*, 4626–4638.

(73) Nová, L.; Uhlík, F.; Košovan, P. Local pH and effective pK_{A} of weak polyelectrolytes - insights from computer simulations. *Phys. Chem. Chem. Phys.* **2017**, *19*, 14376–14387.

(74) Dolce, C.; Mériguet, G. Ionization of short weak polyelectrolytes: when size matters. *Colloid and Polymer Science* **2017**, *295*, 1–9.

(75) Stephan, A.; Batinica, M.; Steiger, J.; Hartmann, P.; Zaucke, F.; Bloch, W.; Fabri, M. LL37:DNA complexes provide antimicrobial activity against intracellular bacteria in human macrophages. *Immunology* **2016**, *148*, 420–432.

(76) Moreno-Angarita, A.; Aragón, C. C.; Tobón, G. J. Cathelicidin LL-37: A new important molecule in the pathophysiology of systemic lupus erythematosus. *Journal of Translational Autoimmunity* **2020**, *3*, 100029.

(77) Jones, G.; Hashim, R.; Power, D. A comparison of the strength of binding of antithrombin III, protamine and poly(l-lysine) to heparin samples of different anicoagulant activities. *Biochimica et Biophysica Acta (BBA) - General Subjects* **1986**, *883*, 69–76.

(78) Sokolowska, E.; Kalaska, B.; Miklosz, J.; Mogielnicki, A. The toxicology of heparin reversal with protamine: past, present and future. *Expert Opinion on Drug Metabolism & Toxicology* **2016**, *12*, 897–909.

(79) Schroeder, M.; Hogwood, J.; Gray, E.; Mulloy, B.; Hackett, A.-M.; Johansen, K. B. Protamine neutralisation of low molecular weight heparins and their oligosaccharide components. *Analytical and Bioanalytical Chemistry* **2010**, *399*, 763–771.

(80) Bromfield, S. M.; Wilde, E.; Smith, D. K. Heparin sensing and binding – taking supramolecular chemistry towards clinical applications. *Chem. Soc. Rev.* **2013**, *42*, 9184–9195.

(81) Martin, P.; Vasilyev, G.; Chu, G.; Boas, M.; Arinstein, A.; Zussman, E. pH-Controlled network formation in a mixture of oppositely charged cellulose nanocrystals and poly(allylamine). *Journal of Polymer Science Part B: Polymer Physics* **2019**, *57*, 1527–1536.

(82) Lacabanne, D.; Boudet, J.; Malär, A. A.; Wu, P.; Cadalbert, R.; Salmon, L.; Allain, F. H.-T.; Meier, B. H.; Wiegand, T. Protein Side-Chain–DNA Contacts Probed by Fast Magic-Angle Spinning NMR. *The Journal of Physical Chemistry B* **2020**, *124*, 11089–11097, PMID: 33238710.

(83) Boukadida, M.; Anene, A.; Jaoued-Grayaa, N.; Chevalier, Y.; Hbaieb, S. Choice of the functional monomer of molecularly imprinted polymers: Does it rely on strong acid-

base or hydrogen bonding interactions? *Colloid and Interface Science Communications* **2022**, *50*, 100669.

(84) Vasiliu, T.; Cojocaru, C.; Rotaru, A.; Pricope, G.; Pinteala, M.; Clima, L. Optimization of Polyplex Formation between DNA Oligonucleotide and Poly(L-Lysine): Experimental Study and Modeling Approach. *International Journal of Molecular Sciences* **2017**, *18*, 1291.

(85) Lunkad, R.; Murmiliuk, A.; Hebbeker, P.; Boublík, M.; Tošner, Z.; Štěpánek, M.; Košovan, P. Quantitative prediction of charge regulation in oligopeptides. *Molecular Systems Design & Engineering* **2021**, *6*, 122–131.

(86) Lunkad, R.; Murmiliuk, A.; Tošner, Z.; Štěpánek, M.; Košovan, P. Role of pKA in Charge Regulation and Conformation of Various Peptide Sequences. *Polymers* **2021**, *13*, 214.

(87) Reed, C. E.; Reed, W. F. Monte Carlo study of titration of linear polyelectrolytes. *The Journal of Chemical Physics* **1992**, *96*, 1609–1620.

(88) Weik, F.; Weeber, R.; Szuttor, K.; Breitsprecher, K.; de Graaf, J.; Kuron, M.; Landsgesell, J.; Menke, H.; Sean, D.; Holm, C. ESPResSo 4.0 – an extensible software package for simulating soft matter systems. *The European Physical Journal Special Topics* **2019**, *227*, 1789–1816.

(89) Weeber, R.; Grad, J.-N.; Beyer, D.; Blanco, P. M.; Kreissl, P.; Reinauer, A.; Tischler, I.; Košovan, P.; Holm, C. In *Comprehensive Computational Chemistry*, 1st ed.; Yáñez, M., Boyd, R. J., Eds.; Elsevier: Oxford, 2024; pp 578–601.

TOC Graphic